

BER Performance for Downlink MC-CDMA Systems over Rician Fading Channels

Zhihua Hou

*Positioning & Wireless Technology Centre (PWTC), School of Electrical & Electronic Engineering, Nanyang Technological University, 50 Nanyang Drive, Singapore 637553
Email: houzhuhua@mail.ntu.edu.sg*

Vimal K. Dubey

*School of Electrical & Electronic Engineering, Nanyang Technological University, 50 Nanyang Avenue, Singapore 639798
Email: evkdubey@ntu.edu.sg*

Received 30 July 2003; Revised 1 April 2004

We consider downlink multicarrier code-division multiple-access (MC-CDMA) systems using binary phase-shift keying (BPSK) modulation scheme and maximal ratio combining (MRC) in frequency-selective Rician fading channels. A time-domain method to obtain bit error rate (BER) by calculating moment generating function (MGF) of the decision variable for a tapped-delay-line channel model is proposed. This method does not require any assumption regarding the statistical or spectral distribution of multiple access interference (MAI), and it is also not necessary to assume that the fading encountered by the subcarriers is independent of each other. The analytical formula is also verified by simulations.

Keywords and phrases: frequency-selective Rician fading channels, MC-CDMA, moment generating function, performance analysis, BER for downlink MC-CDMA systems over Rician fading channels.

1. INTRODUCTION

MC-CDMA systems, based on the combination of code-division multiple-access (CDMA) and orthogonal frequency-division multiplexing (OFDM) techniques, were proposed in 1993 [1]. The multicarrier CDMA schemes can be categorized into two groups: MC-CDMA and MC-DS-CDMA [2]. Due to the attractive features like efficient frequency diversity and high bandwidth efficiency [3], MC-CDMA has received greater attention. Furthermore, MC-CDMA outperforms direct sequence CDMA (DS-CDMA) and MC-DS-CDMA in terms of BER performance over the downlink. Hence, MC-CDMA appears to be a suitable candidate for supporting multimedia services in mobile radio communications for the downlink.

Most of the previous papers [1, 4, 5], which investigated the performance of the MC-CDMA systems, assumed that the fading in different subcarriers is independent of each other, so that the variance of the interference can be approximated by using the central limit theorem. Nevertheless, the assumption is not guaranteed in practice, as the fading of the subcarriers is usually correlated due to insufficient frequency separation between the subcarriers. Also, the assumption of independent fading characteristic implies a frequency-selective fading channel at each subcarrier, since it

requires sufficient independent paths uniformly distributed over the symbol duration [3], which contradicts the assumption of flat fading at each subcarrier. An exact error floor without taking into account the noise term is obtained in [6] under the assumption of exponential multipath intensity profile. In [7], a closed-form BER expression for a synchronous MC-CDMA in the uplink has been obtained assuming independent fading among subcarriers. In [8], a performance evaluation using characteristic method is proposed for MC-DS-CDMA systems. All the above-mentioned papers consider Rayleigh fading channels, and the results for other more general channel models are not available. In this paper, we propose a time-domain approach instead of usual frequency-domain approach to obtain the error performance of downlink MC-CDMA with maximal ratio combining (MRC) in correlated Rician fading channels. We can obtain an exact BER performance without having to make any assumption about the MAI distribution by calculating the moment generating function (MGF). It is also not necessary to assume that the fading of the subcarriers is independent of each other. In addition, it is not necessary to make assumption regarding the correlation property of the spreading sequence. The closed-form error performance may provide helpful insights relevant to designing the spreading sequences for MC-CDMA systems and may

lead to an improved performance for MRC which has been shown to suffer severe MAI when the number of users is large.

Notation

$(\cdot)^*$, $(\cdot)^T$, and $(\cdot)^H$ denote complex conjugate, transpose, and conjugate transpose operation, respectively. Vectors and matrices are represented in bold. $E[\cdot]$ denotes expectation. $|\cdot|$ stands for the norm of a complex variable or a vector. $\text{Re}[\cdot]$ and $\text{Im}[\cdot]$ correspond to the real and imaginary parts of a complex number. Matlab's notation $\text{FFT}(\cdot, n)$ and $\text{IFFT}(\cdot, n)$ denote n -point fast Fourier transform (FFT) and inverse FFT (IFFT). $\langle \mathbf{x} \cdot \mathbf{y} \rangle$ stands for point multiplication between two vectors. \otimes represents circular convolution. $(m)_N = \text{mod}(m, N)$. $N(\mu, \sigma^2)$ denotes normal distributed random variable with μ as mean and σ^2 as variance, respectively. $\det(\cdot)$ denotes the determinant of a matrix.

2. SYSTEM MODEL

2.1. Transmitter

We consider the system proposed in [1] and assume that there are Ku active users in a downlink. At the transmitter side, the spreading binary data stream is serial-to-parallel converted to N parallel substreams. All the data in N subcarriers are modulated in baseband using binary phase-shift keying (BPSK) by the means of the inverse discrete Fourier transform (IDFT). The resultant signals are then converted back into serial data. The guard interval is inserted between symbols to avoid intersymbol interference (ISI) caused by multipath fading, and finally the signal is transmitted after radio frequency (RF) upconversion. Let $a_k(q)$ and $\{c_{k,i}\}_{i=1}^N$ denote the q th data bit and the spreading sequence of user k , respectively. The equivalent lowpass transmitted signal for user k can be expressed as [3]

$$S^k(t) = \sum_{q=-\infty}^{+\infty} \sum_{i=0}^{N-1} \sqrt{\frac{E_b}{N}} a_k(q) c_{k,i} p_b(t - qT_b) e^{j2\pi i \Delta f (t - qT_b)}, \quad (1)$$

where E_b is the power of the data bit and assumed to be the same for all users, $p_b(t)$ is a rectangular pulse defined in $[0, T_b]$ with T_b denoting the bit duration, and $\Delta f = 1/T_b$ is the minimum subcarrier separation.

2.2. Channel model

We consider a slowly varying frequency-selective Rician fading channel. The channel is modeled as a tapped delay line (TDL) having the following baseband equivalent impulse response [9]:

$$c(t) = \sum_{l=0}^{L_1-1} b(l) \delta(t - lT_c), \quad (2)$$

where $\delta(\cdot)$ is the Dirac delta function, L_1 is the number of resolvable paths of the channel, T_c is the chip duration, $b(l)$

is the l th path gain which is a complex Gaussian random process with zero mean (Rayleigh) or nonzero mean (Rician) and are mutually independent for different l . The Rician probability density function (PDF) is obtained as the PDF of $|b(l)| = \sqrt{B_{lx}^2 + B_{ly}^2}$, where $B_{lx} \sim N(\mu_{lx}, \sigma_l^2)$, $B_{ly} \sim N(\mu_{ly}, \sigma_l^2)$, and B_{lx}, B_{ly} are independent. The Rician K -factor is defined as the ratio of signal power in dominant component over the (local-mean) scattered power. We have

$$K_l = \frac{u_{lx}^2 + u_{ly}^2}{2\sigma_l^2}. \quad (3)$$

Since only the nonzero paths need to be considered, we define $\{v_l\}_{l=0}^{L_1-1}$ as the propagation delay for the nonzero paths normalized by the sample interval, and σ_l^2 as the variance, L is the number of the nonzero paths.

In the frequency domain, all subcarriers are assumed to experience flat but correlated fading. The channel gain for the i th subcarrier is $h_i = \rho_i e^{j\phi_i}$, where ρ_i is Rician distributed with $E[\rho_i^2] = 1$. It has been shown in [10] that

$$h_i = \sum_{l=0}^{L_1-1} b(l) \exp\left(\frac{-j2\pi i l}{N}\right) \quad (i = 0, 1, \dots, N-1). \quad (4)$$

The received signal can be written as

$$r(t) = \sum_{q=-\infty}^{\infty} \sqrt{\frac{E_b}{N}} \sum_{k=1}^{Ku} a_k(q) p_b(t - qT_b) \times \sum_{i=0}^{N-1} \rho_i c_{k,i} e^{j[2\pi i \Delta f (t - qT_b) + \phi_i]} + n(t), \quad (5)$$

where $n(t)$ is additive white Gaussian noise (AWGN) having a double-sided power spectrum density of $N_0/2$ for both real and imaginary components.

2.3. Receiver

At the receiver, the RF signal is first converted to baseband signal. After the portion of the signal corresponding to the prefix is removed, DFT is performed on the signal samples. A coherent correlation receiver with MRC is then used. As the focus of this paper is on the evaluation of BER, we assume perfect subcarrier synchronization with no frequency offset and no nonlinear distortion and also assume perfect subcarrier amplitude/phase estimation. Assuming user u is the desired user, the decision variable of the zeroth data bit is given by

$$Z_u(0) = \text{Re} \left\{ \sum_{i=0}^{N-1} \rho_i c_{u,i} \frac{1}{T_b} \int_0^{T_b} r(t) e^{-j(2\pi i \Delta f t + \phi_i)} dt \right\}. \quad (6)$$

3. PERFORMANCE ANALYSIS

We aim at obtaining a concise form of the decision variable for further processing. With the knowledge that there are usually only a few active taps compared to the number

of subcarriers, the idea is to transform the calculation of the decision variable from the frequency domain to the time domain by applying discrete Parseval's theorem, so that the MGF of the decision variable can be derived. The exact BER is then obtained from the MGF by the Laplace inversion integral or numerical methods.

Assuming the length of the cyclic prefix is longer than the length of the channel impulse response, so that there is no ISI. Here we discuss real spreading codes, which are commonly used in practice, however, extension to complex-valued codes is straightforward. The power loss due to the cyclic prefix is not considered in the analysis. The decision variable of the zeroth data bit in (6) with proper sampling time can be written as

$$Z_u(0) = \text{Re} \left\{ \sqrt{\frac{E_b}{N}} \sum_{i=0}^{N-1} \beta_{ui} h_i h_i^* + \sum_{i=0}^{N-1} c_{u,i} n_i h_i^* \right\}, \quad (7)$$

where $\beta_{ui} = a_u(0) + \sum_{k=1, k \neq u}^{K_u} a_k(0) c_{k,i} c_{u,i}$ ($i = 0, 1, \dots, N-1$), n_i corresponds to the complex additive Gaussian noise at the i th subcarrier.

In order to normalize the AWGN noise, a factor equal to $\sqrt{2/N_0}$ is multiplied to (7). We obtain

$$Z_u(0) = \text{Re} \left\{ \sqrt{\frac{2\gamma_b}{N}} \sum_{i=0}^{N-1} \beta_{ui} h_i h_i^* + \sum_{i=0}^{N-1} c_{u,i} \tilde{n}_i h_i^* \right\}. \quad (8)$$

After normalization, the \tilde{n}_i in (8) is zero-mean, complex Gaussian random variable with a variance of $\sigma_n^2 = 1$ for the real and imaginary components, respectively, and the ratio $\gamma_b = E_b/N_0$ represents the signal-to-noise ratio (SNR) per bit.

Since the noise is AWGN, the multiplication of the noise by spreading codes of the desired user will not change the distribution of the noise. The AWGN noise in the frequency domain is the DFT of the normalized AWGN noise in the time domain $\eta(i)$ multiplied by $1/\sqrt{N}$, where $\eta(i)$ is actually $n(t)$ sampled at the rate of $1/T_c$:

$$\tilde{n}_i = \frac{1}{\sqrt{N}} \sum_{n=0}^{N-1} \eta(n) \exp\left(\frac{-j2\pi in}{N}\right) \quad (i = 0, 1, \dots, N-1). \quad (9)$$

Assume \mathbf{y} is the corresponding signal of $\boldsymbol{\beta}_u$ in the time domain given the value $\mathbf{y} = \text{IFFT}(\boldsymbol{\beta}_u, N)$, \mathbf{x} is the signal corresponding to $\langle \boldsymbol{\beta}_u \cdot \mathbf{h} \rangle$ in the time domain, that is $\mathbf{x} = \text{IFFT}(\langle \boldsymbol{\beta}_u \cdot \mathbf{h} \rangle, N)$. The multiplication of the DFT of two sequences is equivalent to the circular convolution of the two sequences in the time domain [11], the relationship between \mathbf{x} and \mathbf{y} can be thus expressed as

$$\begin{aligned} x(i) &= y(i) \otimes b(i) = \sum_{m=0}^{N-1} b(m) y(i-m)_N \\ &= \sum_{m=0}^{L-1} b(v_m) y(i-v_m)_N, \quad i = 0, 1, \dots, N-1. \end{aligned} \quad (10)$$

Applying discrete Parseval's theorem [11], the summation in the frequency domain in (8) can be converted to the summation in the time domain. Omitting a factor equal to \sqrt{N} , the decision variable in (8) can be rewritten in the time domain as

$$Z_u(0) = \text{Re} \left\{ \sqrt{2\gamma_b} \sum_{i=0}^{N-1} x(i) b(i)^* + \sum_{i=0}^{N-1} \eta(i) b(i)^* \right\}. \quad (11)$$

From (10) and (11), the decision variable in the time domain can be obtained as

$$\begin{aligned} Z_u(0) &= \text{Re} \left\{ \sqrt{2\gamma_b} \sum_{i=0}^{L-1} \sum_{m=0}^{L-1} b(v_m) y(v_i - v_m)_N b(v_i)^* \right. \\ &\quad \left. + \sum_{i=0}^{L-1} \eta(v_i) b(v_i)^* \right\}. \end{aligned} \quad (12)$$

For $a_u(0) = 1$, an error occurs if $Z_u(0) < 0$. For $a_u(0) = -1$, an error occurs if $Z_u(0) > 0$.

The decision variable $Z_u(0)$ is conditioned on the channel coefficients $\{b(v_i)\}_{i=0}^{L-1}$ and the user data $\{a_k(0)\}_{k=1}^{K_u}$. We compute the BER by first averaging over $\{b(v_i)\}_{i=0}^{L-1}$ and then over $\{a_k(0)\}_{k=1}^{K_u}$. In order to obtain an expression of exact error performance, we calculate the Laplace transform of $Z_u(0)$ conditioned on $\{a_k(0)\}_{k=1}^{K_u}$, $\Phi(s) = E(e^{-sZ})$, that is, the MGF of the decision variable $Z_u(0)$. Usually it is not an easy task to calculate the MGF for a random vector since it is by definition the mean of an exponential function of the random variables involved. This generally requires the calculation of multidimensional integral and the knowledge of the joint probability density of the random variables. In this case, since the calculation is converted to the time domain, the channel coefficients $\{b(v_i)\}_{i=0}^{L-1}$ for different paths are statistically independent Gaussian random variables [9] and the exponential of the function turns out to be a noncentral Gaussian quadratic form. The MGF can be calculated as (see the appendix for details)

$$\Phi(-s) = \frac{\exp\left(\sum_{m=1}^M b_m^2 s \lambda_m / (1 - s \lambda_m)\right)}{\prod_{m=1}^M (1 - s \lambda_m)^{w_m}}, \quad (13)$$

where λ_m , for $m = 1, \dots, M$, are distinct eigenvalues of \mathbf{A} defined in (A.10) where M is the total number of distinct eigenvalues, w_m is the multiplicity of the eigenvalue λ_m , b_m is given by (A.14). It is clear that $(-1/\lambda_1, \dots, -1/\lambda_M)$ are the M distinct poles of the MGF $\Phi(s)$ of $Z_u(0)$ conditioned on $\{a_k(0)\}_{k=1}^{K_u}$.

3.1. Closed-form expression

If an exact calculation of $P(Z_u(0) < 0)$ is sought, a common starting point is the Laplace inversion formula [9]

$$\begin{aligned} P_{e,u} |_{a_u(0)=1, \{a_k(0)\}_{k=1, k \neq u}^{K_u}} &= P(Z_u(0) |_{a_u(0)=1, \{a_k(0)\}_{k=1, k \neq u}^{K_u}} \leq 0) \\ &= \frac{1}{2\pi j} \int_{c-j\infty}^{c+j\infty} \Phi(s) \frac{ds}{s}, \end{aligned} \quad (14)$$

where c is a small positive constant between zero and the smallest positive pole of $\Phi(s)/s$.

This complex contour integral might be evaluated exactly by calculating the residues of $\Phi(s)/s$ [12] over the poles in the right-hand side of the complex s -plane. Since $\Phi(s)$ contains essential singularities which make the residue evaluation very difficult, power series expansion is applied to solve the problem instead. Assuming that among the M distinct poles of $\Phi(s)$ (13), M_1 of them are positive. Following the method described in [13], we obtain a closed-form expression for (14) as

$$P_{e,u} |_{a_u(0)=1, \{a_k(0)\}_{k=1, k \neq u}^{K_u}} = \sum_{k=1}^{M_1} \left(\prod_{m=1, m \neq k}^M \left(\left(\frac{\lambda_k}{\lambda_k - \lambda_m} \right)^{w_m} \exp \left(\frac{b_m^2 \lambda_m}{\lambda_k - \lambda_m} \right) \right) \right) \cdot \exp(-b_k^2) \cdot \left(\sum_{n=0}^{\infty} \sum_{r_k=0}^{n+w_k-1} \frac{b_k^{2n} G_k^{(r_k)}(\lambda)}{n! r_k! (-\lambda_k)^{r_k}} \right), \quad (15)$$

where

$$G_k^{(r)}(\lambda) = \left[\sum_{r_1=0}^{r-1} \binom{r-1}{r_1} g_k^{(r-1-r_1)}(\lambda) \cdot \sum_{r_2=0}^{r_1-1} \binom{r_1-1}{r_2} g_k^{(r_1-1-r_2)}(\lambda) \cdots \right]. \quad (16)$$

In (16), $g_k^{(n)}(\lambda)$ is given by

$$g_k^{(n)}(\lambda) = \sum_{m=1, m \neq k}^M \left[n! \left(\frac{\lambda_k \lambda_m}{\lambda_k - \lambda_m} \right)^{n+1} \left(w_m + (n+1) \frac{b_m^2 \lambda_k}{\lambda_k - \lambda_m} \right) \right]. \quad (17)$$

3.2. Numerical method

Equation (15) gives a general closed-form BER expression for MC-CDMA systems over arbitrary Rician multipath fading channels. Since (15) is derived using the fast-convergent power series expansion of the MGF about its positive poles, it is expected to converge rapidly with respect to the index n . However, as shown in [13], the series (15) converges more slowly as the Rician K -factor increases, therefore it is more suitable for analysis of Rician fading channels with a relatively small K -factor, for example, $K \leq 7$ dB. To achieve a more convenient solution to this problem, a different approach towards the exact calculation of (14) is used instead [14].

Since the left-hand side of (14) is a real quantity, we can write

$$P_{e,u} |_{a_u(0)=1, \{a_k(0)\}_{k=1, k \neq u}^{K_u}} = \frac{1}{2\pi} \int_{-\infty}^{\infty} \frac{\Phi(c + j\omega)}{c + j\omega} d\omega = \frac{1}{2\pi} \int_{-\infty}^{\infty} \frac{c \operatorname{Re} \{ \Phi(c + j\omega) \} + \omega \operatorname{Im} \{ \Phi(c + j\omega) \}}{c^2 + \omega^2} d\omega. \quad (18)$$

The change of variable $\omega = c\sqrt{1-x^2}/x$ yields

$$P_{e,u} |_{a_u(0)=1, \{a_k(0)\}_{k=1, k \neq u}^{K_u}} = \frac{1}{2\pi} \int_{-1}^1 \left\{ \operatorname{Re} \left[\Phi \left(c + jc \frac{\sqrt{1-x^2}}{x} \right) \right] + \frac{\sqrt{1-x^2}}{x} \operatorname{Im} \left[\Phi \left(c + jc \frac{\sqrt{1-x^2}}{x} \right) \right] \right\} \frac{dx}{\sqrt{1-x^2}}. \quad (19)$$

Finally, using a Gauss-Chebyshev quadrature rule with an even number ν of nodes, we have

$$P_{e,u} |_{a_u(0)=1, \{a_k(0)\}_{k=1, k \neq u}^{K_u}} = \frac{1}{\nu} \sum_{k=1}^{\nu/2} \left\{ \operatorname{Re} [\Phi(c + jc\tau_k)] + \tau_k \operatorname{Im} [\Phi(c + jc\tau_k)] \right\} + E_\nu, \quad (20)$$

where $\tau_k = \tan((2k-1)\pi/(2\nu))$ and the error term E_ν vanishes as $\nu \rightarrow \infty$. To achieve the desired degree of accuracy, it is practical increasing values of ν and accepting the result when it does not change significantly. In general, 32 to 64 nodes are sufficient to obtain an accuracy better than 10^{-5} . The value of c affects the number of nodes necessary to achieve a pre-assigned accuracy. The detailed discussion concerning the selection of c can be found in [14]. In our numerical results, we assume $\nu = 64$, and c is set equal to one half the smallest real part of the poles of $\Phi(s)$. However, even with a suboptimum choice of c , the value of ν does not grow large enough as to become unmanageable.

In the above section, a closed-form expression and a numerical method are given to obtain the error probability conditioned on the user data based on the MGF. For coherent detection, we have

$$P_{e,u} |_{a_u(0)=1, \{a_k(0)\}_{k=1, k \neq u}^{K_u}} = P_{e,u} |_{a_u(0)=-1, \{a_k(0)\}_{k=1, k \neq u}^{K_u}}. \quad (21)$$

By averaging the conditioned BER (15) or (20) over $\{a_k(0)\}_{k=1, k \neq u}^{K_u}$ which are independent and identically distributed binary random variables, we obtain the BER of the user u :

$$P_{e,u} = \frac{1}{2^{K_u-1}} \sum_{a_1(0) \in \{1, -1\}} \cdots \sum_{a_{k \neq u}(0) \in \{1, -1\}} \cdots \times \sum_{a_{K_u}(0) \in \{1, -1\}} P_{e,u} |_{a_u(0)=1, \{a_k(0)\}_{k=1, k \neq u}^{K_u}}. \quad (22)$$

The average BER of all users is given by

$$P_e = \frac{1}{K_u} \sum_{i=1}^{K_u} P_{e,i}. \quad (23)$$

As the computational complexity to evaluate (22) increases exponentially with the number of users, the proposed approach is appropriate for systems with relatively small number of users, say $Ku < 20$. When the number of users is large, we may resort to traditional Gaussian approximation. In the following section, we propose a simple evaluation method to remedy this problem.

3.3. Gaussian approximation method for large number of users

From (7), the decision variable of the desired user can be rewritten as

$$Z_u(0) = D_u + I_u + N_u, \quad (24)$$

where

$$D_u = \sqrt{\frac{E_b}{N}} a_u(0) \sum_{i=0}^{N-1} |h_i|^2, \quad (25)$$

$$I_u = \sqrt{\frac{E_b}{N}} \sum_{i=0}^{N-1} |h_i|^2 \sum_{k=1, k \neq u}^{K_u} a_k(0) c_{u,i} c_{k,i}, \quad (26)$$

$$N_u = \text{Re} \left[\sum_{i=0}^{N-1} c_{u,i} h_i^* n_i \right]. \quad (27)$$

The term D_u is the desired output. I_u corresponds to the MAI component. N_u is the noise term contributed by AWGN. Due to the equal power, equally likely, antipodal data modulation $a_k(0)$ in (26), we apply the central limit theorem and approximate $g_{u,i} = \sum_{k=1, k \neq u}^{K_u} a_k(0) c_{u,i} c_{k,i}$ ($i = 0, 1, \dots, N-1$) as a zero mean Gaussian random variable. Note that $g_{u,i}$ is correlated between subcarriers. The covariance matrix M_u is an $N \times N$ matrix with each element given by $M_u(i1, i2) = \sum_{k=1, k \neq u}^{K_u} c_{u,i1} c_{k,i1} c_{u,i2} c_{k,i2}$.

The decision variable conditioned on $\{h_i\}_{i=0}^{N-1}$ is a Gaussian random variable with

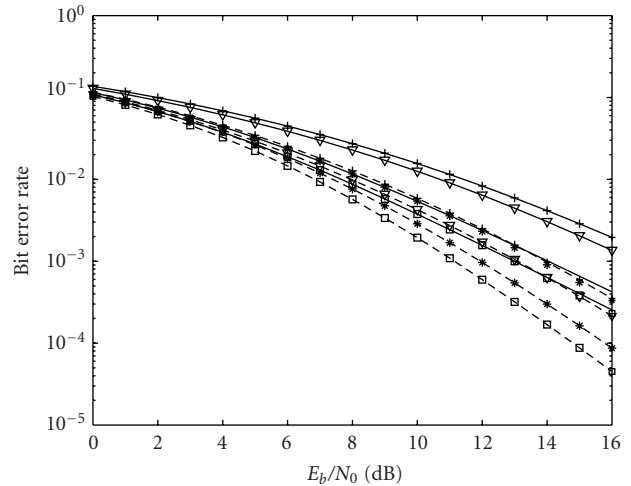
$$E(D_u) = \sqrt{\frac{E_b}{N}} a_u(0) \sum_{i=0}^{N-1} |h_i|^2 = \sqrt{\frac{E_b}{N}} a_u(0) \sum_{i=0}^{N-1} \rho_i^2, \quad (28)$$

$$\begin{aligned} \text{var}(I_u) &\approx \frac{E_b}{N} \sum_{i1=0}^{N-1} \sum_{i2=0}^{N-1} |h_{i1}|^2 |h_{i2}|^2 M_u(i1, i2) \\ &= \frac{E_b}{N} \sum_{i1=0}^{N-1} \sum_{i2=0}^{N-1} \rho_{i1}^2 \rho_{i2}^2 M_u(i1, i2), \end{aligned} \quad (29)$$

$$\text{var}(N_u) = \frac{N_0}{2} \sum_{i=0}^{N-1} |h_i|^2 = \frac{N_0}{2} \sum_{i=0}^{N-1} \rho_i^2. \quad (30)$$

Equation (29) is derived from [15] for the variance of the linear combination of correlated random variables. The probability of error conditioned on $\{\rho_i\}_{i=0}^{N-1}$ is simply given by

$$P[e|\boldsymbol{\rho}] = \frac{1}{2} \text{erfc} \left(\sqrt{\frac{E(D_u)}{\text{var}(I_u) + \text{var}(N_u)}} \right). \quad (31)$$



— Closed-form method, 2-ray
 --- Closed-form method, 3 p
 * Numerical method, $K = 0.2$, 1 u
 + Numerical method, $K = 0.2$, 10 u
 □ Numerical method, $K = 1$, 1 u
 ▽ Numerical method, $K = 1$, 10 u

FIGURE 1: Theoretical BER of MC-CDMA for the 2-ray ($K_0 = K_1 = K$) and 3-path channel models ($K_0 = K_1 = K_2 = K$) using MRC by the closed-form and the numerical method.

The BER for the zeroth data stream is obtained via averaging $P[e|\boldsymbol{\rho}]$ over $\boldsymbol{\rho}$:

$$\begin{aligned} P_e &= \int_0^\infty \int_0^\infty \cdots \int_0^\infty p[e|\boldsymbol{\rho}] p \\ &\quad \times (\rho_0, \rho_1, \dots, \rho_{N-1}) d\rho_0 d\rho_1 \cdots d\rho_{N-1}. \end{aligned} \quad (32)$$

Equation (32) can be evaluated by Monte Carlo integration [4, 16].

4. NUMERICAL RESULTS

In this section, we present numerical results. To calculate the BER, it is assumed that the number of subcarriers is 32, and two channel delay profiles are considered, a simple two-ray multipath delay profile often encountered in urban and hilly areas [14], and a three-path channel with linear delay power profile [17]. For the two-ray channel, we assume $\nu_0 = 0, \nu_1 = 14$. Furthermore, Walsh Hadamard codes are used as the spreading codes.

For the channels and the signals described above, we can compute the BER based on the closed-form expression given by (15) and (22) and the numerical method (20). Shown in Figure 1, the results obtained by the two methods match very well as long as the value of n is sufficiently large. To check how quickly the infinite series in (15) converges with respect to n , we give the BER values based on the truncated series for the index n summing up from 0 to n_{\max} in Tables 1 and 2 for two-ray and three-path channels. The BER for n_{\max} is obtained by setting n_{\max} large enough in (15), so that the first

TABLE 1: BER values with truncated series for the 2-ray channel: $Ku = 1$, SNR = 0 dB.

n_{\max}	K -factor		
	$K = 0.2$	$K = 1$	$K = 4.5$
5	0.114438389	0.107710909	0.0670963590
10	0.114438390	0.107723090	0.0915495818
∞	0.114438390	0.107723090	0.0917931623
Numerical	0.114438390	0.107723090	0.0917931623

TABLE 2: BER values with truncated series for the 3-path channel: $Ku = 1$, SNR = 0 dB.

n_{\max}	K -factor		
	$K = 0.2$	$K = 1$	$K = 2.8$
10	0.108401585	0.117951253	0.146651024
15	0.108401585	0.102827722	0.128790431
20	0.108401585	0.102830484	0.103149956
∞	0.108401585	0.102830484	0.0939229789
Numerical	0.108401585	0.102830484	0.0939229789

nine significant digits for each BER value converge. It is also shown in the tables that the results of the closed-form expression conform exactly with those computed by the numerical method. The results in Tables 1 and 2 also show that the series in (15) converges very rapidly for a relatively small K -factor, and $n_{\max} = 5$ –10 may be accurate enough for practical interest. For large K -factors, it requires $n_{\max} = 15$ –30 to get an accurate approximation. Since the numerical method appears more computationally efficient compared with the closed-form expression especially when the K -factor is large, in Figures 2–7, the analytical results are obtained using the numerical method.

The results of our proposed time-domain method described herein are verified by comparing with the Monte Carlo simulations. In Figures 2 and 3, the K -factors for different taps are equal, while in Figure 4, the K -factors for each tap are different. In all these cases, the simulation results agree very well with the theoretical results obtained by the technique proposed in this paper. The simulation results are based on the calculation of the decision variable for each bit, and averaging the results over large number of bits (say 100 000 bits). Figure 5 shows the accuracy of our low-complexity method proposed in Section 3.3. The results indicate that our low-complexity method gives quite a good approximation as compared with the accurate result, and the accuracy improves when the number of users is high.

Next, the effect of the Rician K -factor on the BER performance is investigated using the analytical formula derived in Section 3. The Rician K -factor is defined as the ratio of signal power in dominant component over the (local-mean) scattered power which corresponds to a deterministic strong wave received. It is natural to expect a better performance for larger values of K . From the analytical results shown in (Figure 6), it can be seen that the performance improvement due to the increase in K is evident when the number of user is small (i.e., MAI is not dominant), while for 20 users

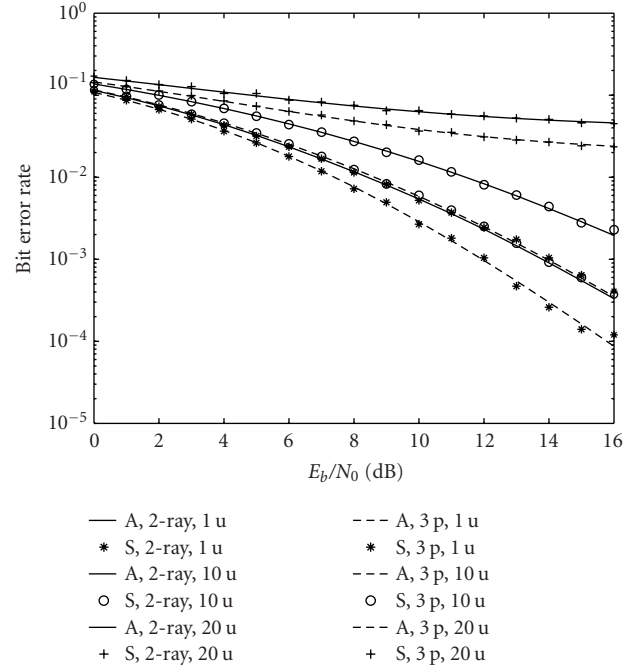


FIGURE 2: BER of MC-CDMA for the 2-ray ($K_0 = K_1 = K = 0.2$) and 3-path channel models ($K_0 = K_1 = K_2 = K = 0.2$) using MRC. (A: theoretical results; S: simulation results.)

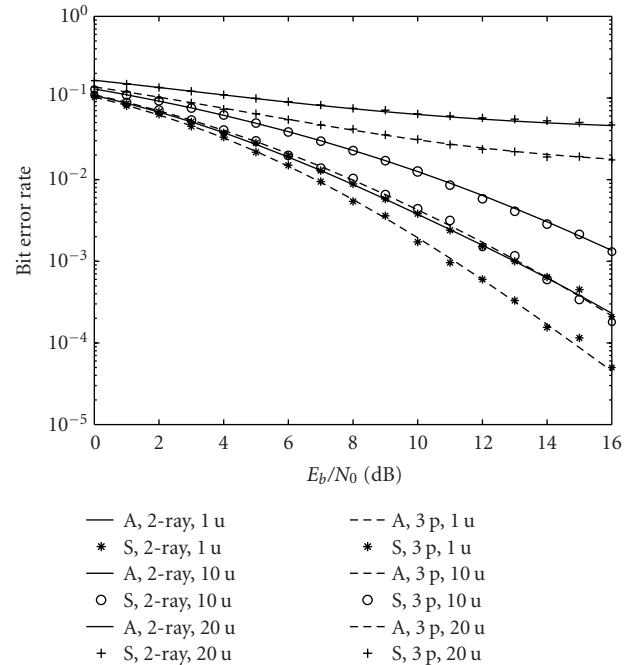


FIGURE 3: BER of MC-CDMA for the 2-ray ($K_0 = K_1 = K = 1$) and 3-path channel models ($K_0 = K_1 = K_2 = K = 1$) using MRC. (A: theoretical results; S: simulation results.)

(where MAI dominates), there is no difference between the BER performance for different values of K (i.e., $K = 0.2$, $K = 1$, and $K = 10$). For this case, MAI tends to be so severe and it becomes the dominant factor in determining the

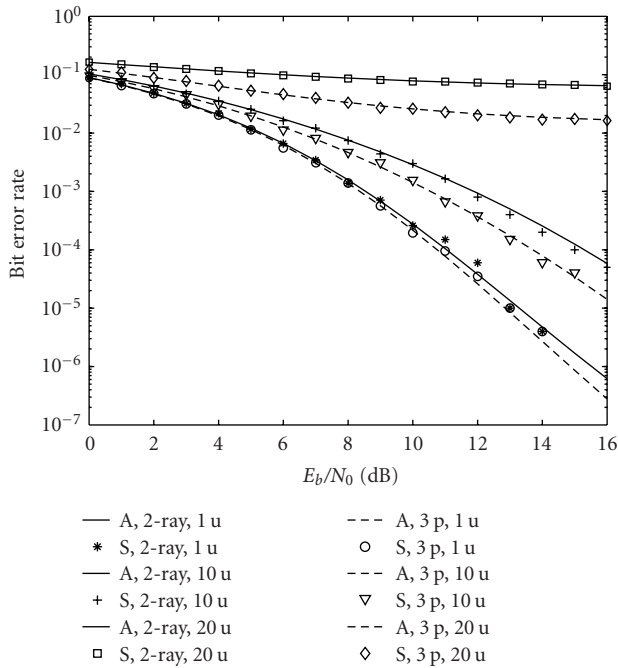


FIGURE 4: BER of MC-CDMA using MRC for the 2-ray channel model ($K_0 = 10, K_1 = 4$) and for the 3-path channel model ($K_0 = 10, K_1 = 2.5, K_2 = 0$). (A: theoretical results; S: simulation results.)

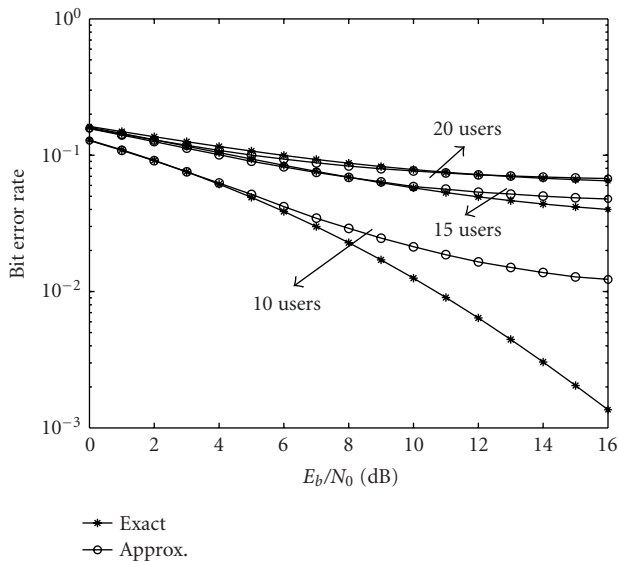


FIGURE 5: BER of MC-CDMA system with MRC versus SNR for the 2-ray channel model: $\nu_0 = 0, \nu_1 = 14$, and $K_0 = K_1 = 1$.

system performance. Simulation results are also given to validate the analytical results. Figure 7 shows the BER comparison for various K when SNR equals 10 dB for 1, 10, and 20 users. A distinct variation can be seen when the number of users is small, while for 20 users, there is hardly any variation in the BER as MAI dominates the performance in this case.

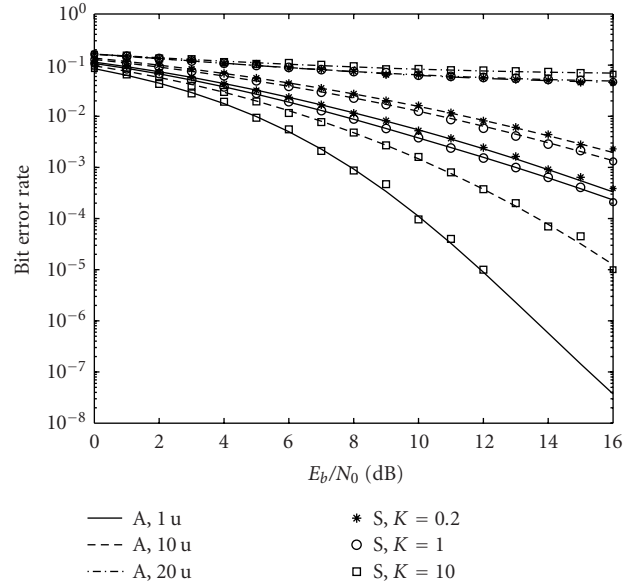


FIGURE 6: BER of MC-CDMA system versus SNR with various number of users and K -factor for the 2-ray channel model: $\nu_0 = 0, \nu_1 = 14, K_0 = K_1 = K$. (A: theoretical results; S: simulation results.)

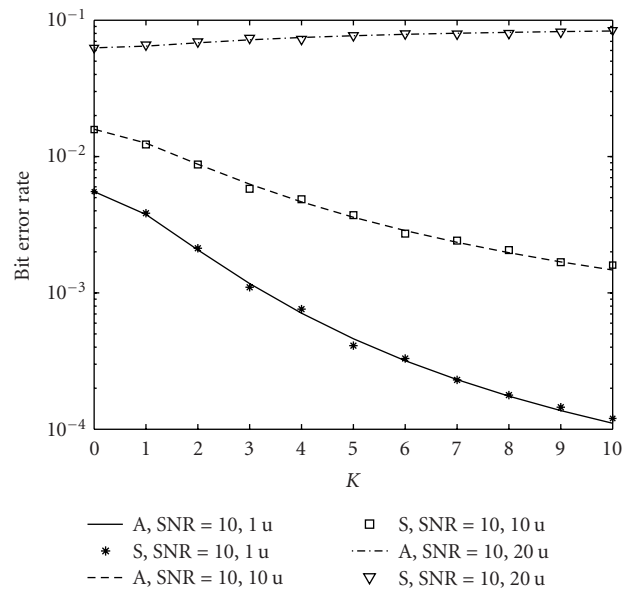


FIGURE 7: BER of MC-CDMA system versus K -factor, SNR = 10 dB for the 2-ray channel model: $\nu_0 = 0, \nu_1 = 14, K_0 = K_1 = K$. (A: theoretical results; S: simulation results.)

5. CONCLUSION

In this paper, we have proposed an accurate and simple method to calculate the performance of MC-CDMA systems with MRC combining scheme over downlink correlated Rician fading channels. A general algorithm is proposed to

calculate the moment generating function by expressing the decision variables in Gaussian quadratic forms. Based on the moment generating function, an exact BER is obtained in the time domain. However, the complexity of this method increases exponentially with the number of users. To alleviate this problem, we have also proposed a low-complexity approximate BER evaluation method by using the Monte Carlo integration. The results obtained by the analytical formula have been thoroughly verified by computer simulations.

APPENDIX

DERIVATION OF MGF

In this appendix, we show the detailed derivation of (13) starting from (12). The MGF of the decision variable for frequency-selective channels under Rician distribution is derived. The decision variable $Z_u(0)$ in (12) can be rewritten as

$$Z_u(0) = \text{Re} \left\{ \sqrt{2\gamma_b} \left[\sum_{i=0}^{L-1} |b(v_i)|^2 y(0) + \sum_{i=0}^{L-1} \sum_{m=0, m \neq i}^{L-1} b(v_i)^* b(v_m) y_{i,m} \right] + \sum_{i=0}^{L-1} \eta(v_i) b(v_i)^* \right\}, \quad (\text{A.1})$$

with $y(v_i - v_m)_N$ denoted by $y_{i,m}$ for simplicity.

If the decision variable in (A.1) is written in vector form, the derivation of the MGF can be expressed more concisely. The vector form of the decision variable for the desired user is given by

$$Z_u(0) = \mathbf{v}^H(0) \mathbf{Q}(0) \mathbf{v}(0), \quad (\text{A.2})$$

where

$$\mathbf{v}(0) = \left[b(v_0) \ b(v_1) \ \cdots \ b(v_{L-1}) \ \eta(v_0) \ \eta(v_1) \ \cdots \ \eta(v_{L-1}) \right]^T. \quad (\text{A.3})$$

$\mathbf{Q}(0)$ is a $2L \times 2L$ matrix defined as

$$\mathbf{Q}(0) = \begin{bmatrix} \mathbf{Q}_1 & 0.5\mathbf{I}_L \\ 0.5\mathbf{I}_L & \mathbf{0}_L \end{bmatrix}, \quad (\text{A.4})$$

where

$$\mathbf{Q}_1 = \sqrt{2\gamma_b} \begin{bmatrix} y(0) & y_{0,1} & y_{0,2} & \cdots & y_{0,L-1} \\ y_{0,1}^* & y(0) & y_{1,2} & \cdots & y_{1,L-1} \\ y_{0,2}^* & y_{1,2}^* & \ddots & \ddots & \vdots \\ \vdots & \vdots & \ddots & \ddots & y_{L-2,L-1} \\ y_{0,L-1}^* & y_{1,L-1}^* & \cdots & y_{L-2,L-1}^* & y(0) \end{bmatrix}. \quad (\text{A.5})$$

In (A.4), $\mathbf{0}_L$ and \mathbf{I}_L are the $L \times L$ zero and identity matrices, respectively.

With the assumption that the channel coefficients $b(l)$ for different paths are statistically independent of each other and the AWGN noise term is independent of the channel impulse response, a simple expression of the covariance matrix of $\mathbf{v}(0)$ is achieved:

$$\mathbf{P}_v = E\{\mathbf{v}(0)\mathbf{v}^H(0)\} = 2 \text{diag} \left(\sigma_0^2, \sigma_1^2, \dots, \sigma_{L-1}^2, \underbrace{1, \dots, 1}_L \right). \quad (\text{A.6})$$

The mean vector of $\mathbf{v}(0)$ is given by

$$\begin{aligned} \boldsymbol{\mu}_v &= E(\mathbf{v}(0)) \\ &= \left[(\mu_{0x} + j\mu_{0y}), (\mu_{1x} + j\mu_{1y}), \dots, \right. \\ &\quad \left. (\mu_{(L-1)x} + j\mu_{(L-1)y}), \underbrace{0, \dots, 0}_L \right]^T. \end{aligned} \quad (\text{A.7})$$

Employing a result for the distribution of a noncentral Gaussian quadratic form [13], the MGF of $Z_u(0)$ in (A.2) can be obtained as

$$\Phi(-s) = \frac{\exp(\boldsymbol{\mu}_v^H \mathbf{F}(s) \boldsymbol{\mu}_v)}{\det(\mathbf{I} - s\mathbf{P}_v^{1/2} \mathbf{Q} \mathbf{P}_v^{1/2})}, \quad (\text{A.8})$$

$$\mathbf{F}(s) = \mathbf{P}_v^{-1/2} ((\mathbf{I} - s\mathbf{P}_v^{1/2} \mathbf{Q} \mathbf{P}_v^{1/2})^{-1} - \mathbf{I}) \mathbf{P}_v^{-1/2}, \quad (\text{A.9})$$

where $\mathbf{P}_v^{-1/2}$ is the inverse of the symmetric square root of \mathbf{P}_v .

To represent the conditioned MGF $\Phi(-s)$ in a more compact form, we define a matrix

$$\mathbf{A} = \mathbf{P}_v^{1/2} \mathbf{Q} \mathbf{P}_v^{1/2} \quad (\text{A.10})$$

and represent its eigendecomposition as $\mathbf{A} = \mathbf{U}_v \boldsymbol{\Lambda}_v \mathbf{U}_v^H$, where

$$\boldsymbol{\Lambda}_v = \text{diag}(\lambda_1, \lambda_2, \dots, \lambda_{2L}) \quad (\text{A.11})$$

is the eigenvalue matrix of \mathbf{A} . Also, we define

$$\tilde{\boldsymbol{\mu}}_v = [\tilde{\mu}_1, \tilde{\mu}_2, \dots, \tilde{\mu}_{2L}]^T = \mathbf{U}_v^H \mathbf{P}_v^{-1/2} \boldsymbol{\mu}_v. \quad (\text{A.12})$$

Equation (A.8) can now be simplified to

$$\begin{aligned} \Phi(-s) &= \frac{\exp(\tilde{\boldsymbol{\mu}}_v^H \boldsymbol{\Lambda}(s) \tilde{\boldsymbol{\mu}}_v)}{\det(\mathbf{I} - s\boldsymbol{\Lambda}_v)} \\ &= \frac{\exp(\sum_{k=1}^{2L} |\tilde{\mu}_k|^2 s \lambda_k / (1 - s \lambda_k))}{\prod_{k=1}^{2L} (1 - s \lambda_k)}, \end{aligned} \quad (\text{A.13})$$

where $\boldsymbol{\Lambda}(s) = (\mathbf{I} - s\boldsymbol{\Lambda}_v)^{-1} - \mathbf{I}$ is a diagonal matrix.

In the case of repeated eigenvalues, the MGF of $Z_u(0)$ is given by (13). In (13)

$$b_m^2 = \sum_{k \in \kappa_m} |\bar{\mu}_k|^2, \quad (\text{A.14})$$

where κ_m denotes the set of k indices associated with the m th distinct eigenvalue.

Here, the MGF of the decision variable for the two-ray channel model is given as an example:

$$\Phi(s) = \frac{e^{-(K_0+K_1)}}{R} e^{2(\sigma_0^2 K_0 M_1 + \sigma_0^2 K_1 M_0 - W)/R}, \quad (\text{A.15})$$

where the coefficients are given by

$$\begin{aligned} R &= c_4 s^4 + c_3 s^3 + c_2 s^2 + c_1 s + 1, \\ c_4 &= \sigma_0^2 \sigma_1^2, \\ c_3 &= -4\sqrt{2\gamma_b} \sigma_0^2 \sigma_1^2 y(0), \\ c_2 &= -(\sigma_0^2 + \sigma_1^2) + 8\gamma_b \sigma_0^2 \sigma_1^2 y(0)^2 - 8\gamma_b \sigma_0^2 \sigma_1^2 |y_{0,1}|^2, \\ c_1 &= 2\sqrt{2\gamma_b} (\sigma_0^2 + \sigma_1^2) y(0), \\ W &= \sqrt{2\gamma_b} s [\mu_{0x} \mu_{1x} \operatorname{Re}(y_{0,1}) + \mu_{0y} \mu_{1x} \operatorname{Im}(y_{0,1}) \\ &\quad + \mu_{0y} \mu_{1y} \operatorname{Re}(y_{0,1}) - \mu_{0x} \mu_{1y} \operatorname{Im}(y_{0,1})]. \end{aligned} \quad (\text{A.16})$$

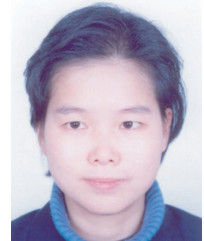
The region of convergence is the vertical strip enclosing the $j\omega$ axis bounded by the closest poles on either side. The BER performance can be obtained through the method described above.

REFERENCES

- [1] N. Yee, J. P. Linnartz, and G. Fettweis, "Multi-carrier CDMA in indoor wireless radio networks," *IEICE Trans. Commun.*, vol. E77-B, no. 7, pp. 900–904, 1994.
- [2] S. Hara and R. Prasad, "Overview of multicarrier CDMA," *IEEE Communications Magazine*, vol. 35, no. 12, pp. 126–133, 1997.
- [3] S. Hara and R. Prasad, "Design and performance of multicarrier CDMA system in frequency-selective Rayleigh fading channels," *IEEE Trans. Vehicular Technology*, vol. 48, no. 5, pp. 1584–1595, 1999.
- [4] E. A. Sourour and M. Nakagawa, "Performance of orthogonal multicarrier CDMA in a multipath fading channel," *IEEE Trans. Communications*, vol. 44, no. 3, pp. 356–367, 1996.
- [5] N. Yee and J. P. Linnartz, "BER of multi-carrier CDMA in an indoor Rician fading channel," in *Proc. 27th Asilomar Conference on Signals, Systems and Computers*, vol. 1, pp. 426–430, Pacific Grove, Calif, USA, November 1993.
- [6] Q. H. Shi and M. Latva-aho, "An exact error floor for downlink MC-CDMA in correlated Rayleigh fading channels," *IEEE Communications Letters*, vol. 6, no. 5, pp. 196–198, 2002.
- [7] Q. H. Shi and M. Latva-aho, "Exact bit error rate calculations for synchronous MC-CDMA over a Rayleigh fading channel," *IEEE Communications Letters*, vol. 6, no. 7, pp. 276–278, 2002.
- [8] B. Smida, C. L. Despina, and G. Y. Delisle, "MC-CDMA performance evaluation over a multipath fading channel using the characteristic function method," *IEEE Trans. Communications*, vol. 49, no. 8, pp. 1325–1328, 2001.

- [9] J. G. Proakis, *Digital Communications*, McGraw-Hill, New York, NY, USA, 4th edition, 2001.
- [10] Y. Li, L. J. Cimini Jr., and N. R. Sollenberger, "Robust channel estimation for OFDM systems with rapid dispersive fading channels," *IEEE Trans. Communications*, vol. 46, no. 7, pp. 902–915, 1998.
- [11] J. G. Proakis and D. G. Manolakis, *Digital Signal Processing*, Prentice-Hall, Englewood Cliffs, NJ, USA, 3rd edition, 1996.
- [12] J. K. Cavers and P. Ho, "Analysis of the error performance of trellis-coded modulations in Rayleigh-fading channels," *IEEE Trans. Communications*, vol. 40, no. 1, pp. 74–83, 1992.
- [13] Y. Ma, T. L. Lim, and S. Pasupathy, "Error probability for coherent and differential PSK over arbitrary Rician fading channels with multiple cochannel interferers," *IEEE Trans. Communications*, vol. 50, no. 3, pp. 429–441, 2002.
- [14] E. Biglieri, G. Caire, G. Taricco, and J. Ventura-Traveset, "Simple method for evaluating error probabilities," *Electronics Letters*, vol. 32, no. 3, pp. 191–192, 1996.
- [15] C. W. Helstrom, *Probability and Stochastic Processes for Engineers*, Macmillan Publishing, New York, NY, USA, 1991.
- [16] X. Gui and T. S. Ng, "Performance of asynchronous orthogonal multicarrier CDMA system in frequency selective fading channel," *IEEE Trans. Communications*, vol. 47, no. 7, pp. 1084–1091, 1999.
- [17] J. K. Cavers, *Mobile Channel Characteristics*, Kluwer Academic, Boston, Mass, USA, 2000.

Zhihua Hou received the B.S. and M.S. degrees from Xi'an Jiaotong University, China, in 1993 and 1996, respectively, both in electrical engineering and information science. She is now pursuing the Ph.D. degree at the School of Electrical and Electronic Engineering, Nanyang Technological University, Singapore. Her research interests include wireless communications, with emphasis on the analysis of wireless digital communications over fading channels, multicarrier and CDMA techniques, channel estimation, and MIMO communication systems.



Vimal K. Dubey received the B.S. (honors) degree in mathematics from the University of Rajasthan, India, the B.E. and M.E. degrees in electrical communication engineering from the Indian Institute of Science, Bangalore, India, and the Ph.D. degree in electrical engineering from McMaster University, Hamilton, Ontario, Canada. He has worked in various research and development laboratories in India for more than ten years. From 1972 to 1976, he was a Research Scientist at DLRL, Hyderabad, India. From 1976 to 1982, he was with DEAL, Dehradun, India, where he conducted research on spread-spectrum systems for satellite communications and transportable troposcatter communication system. From 1982 to 1986, he was a Commonwealth Research Scholar at McMaster University. He joined the School of Electrical and Electronic Engineering, Nanyang Technological University, Singapore, in 1988, where he is now an Associate Professor. His main research interests are in the areas of digital communications, specializing in coding, modulation, and spread-spectrum systems for satellite and wireless communications.

